DOI: https://doi.org/10.24425/amm.2025.154482

MOHD AZRI AZIZI BIN ISMAIL<sup>©1</sup>, YUKI NAKAGAWA<sup>©2</sup>, TAMAKI SHIBAYAMA<sup>©2\*</sup>

# SYNTHESIS OF TITANIUM DIOXIDE-NICKEL/NICKEL OXIDE QUASI CORE-SHELL NANOPARTICLES USING SOLUTION PLASMA

In this study, TiO<sub>2</sub>@Ni/NiO quasi core-shell nanoparticles (NPs) were synthesized using solution plasma for future photocatalytic applications. X-ray diffraction analysis confirmed that all samples contained TiO<sub>2</sub>, Ni, and NiO. Scanning and scanning transmission electron microscopy images revealed that the quasi core-shell NPs were spherical with smooth surfaces and consisted of larger TiO<sub>2</sub> NPs partially covered by smaller Ni/NiO NPs. Transmission electron microscopy images showed degradation of PVP forming visible solid precipitates at 0.25% (w/v) PVP concentration. X-ray photoelectron spectroscope (XPS) analysis indicates that the N 1s peak at 399.3-400.1 eV is contributed bynitrogen atom in the PVP molecule. The optimal PVP concentration was determined to be in the range of 0.05%-0.15% (w/v) PVP; a higher concentration of 0.25% (w/v) PVP led to degradation of PVP. *Keywords:* Titanium dioxide; nickel oxide; polyvinylpyrrolidone; quasi core-shell nanoparticles; solution plasma

#### 1. Introduction

Titanium dioxide (TiO<sub>2</sub>), a well-studied n-type semiconductor, has drawn extensive interest because of its unique photocatalytic properties. With a bandgap of ~3.0 eV, TiO<sub>2</sub> is capable of participating in redox reaction by generating electron-hole pairs upon ultraviolet-light irradiation, making it highly effective for photocatalytic applications [1,2]. Since the breakthrough discovery of photocatalytic decomposition of water using TiO<sub>2</sub> electrodes by Fujishima and Honda in 1972, much research has been devoted to improving the photocatalytic efficiency and further exploring the potential of TiO<sub>2</sub> [3]. The rapid recombination rate of electron-hole pairs can be lowered and the wide bandgap of TiO<sub>2</sub> can be narrowed by constructing n-p heterojunctions using the earth-abundant p-type semiconductor nickel oxide (NiO). This configuration creates an internal electric field that acts as a barrier, increasing the separation and lifetime of charge carriers, thus enhancing photocatalytic performance. TiO<sub>2</sub>@ NiO core-shell nanoparticles (NPs) have been shown to display improved photocatalytic performance compared with that of  $TiO_2$  alone [4-6].

In general, wet chemical approaches to synthesize TiO<sub>2</sub>@ NiO core-shell NPs possess several limitations, including long reaction times, multi-step synthesis, and complex instrumentation requirements [7]. One promising method to synthesize

such structures in a facile manner is solution plasma. Solution plasma is an electrolysis process in which an atmospheric nonequilibrium plasma is generated through electrical discharge of electrodes at room temperature in a liquid environment. In this method, a high-temperature plasma sheath is formed near the cathode by local concentration of current induced by electrothermal instability, causing glow discharge photoemission and dissolution of the electrode to produce NPs [8]. The benefits of solution plasma are simple setup, the ability to synthesize NPs at room temperature, ease of mass production, and its green nature (no toxic chemicals and low energy requirements) [9]. Synthesis of TiO<sub>2</sub> and NiO NPs using solution plasma has been reported, with both anatase and rutile phases of TiO2 being produced [10,11]. However, core-shell NP synthesis using solution plasma is rare because of challenges such as incomplete coverage of the NP core, particle aggregation to form large clusters, and lattice mismatch between constituent materials [12]. Inclusion of a surface modifier such as polyvinylpyrrolidone (PVP) can promote the formation of NPs with a core-shell structure. PVP usually serves as a surface stabilizer, growth modifier, NP dispersant, and reducing agent but can also behave as an effective linker by modifying the interfacial tension between materials. That is, PVP can act as the intermediate layer to promote the selective deposition of the shell material on the surface of the core to form uniform disperse core-shell NPs [13,14].

<sup>\*</sup> Corresponding author: shiba@qe.eng.hokudai.ac.jp



HOKKAIDO UNIVERSITY, GRADUATE SCHOOL OF ENGINEERING, N13 W8, KITA-KU, SAPPORO, HOKKAIDO 060-8628, JAPAN

HOKKAIDO UNIVERSITY, FACULTY OF ENGINEERING, N13 W8, KITA-KU, SAPPORO, HOKKAIDO 060-8628, JAPAN

This study investigates the feasibility of using solution plasma to synthesize TiO<sub>2</sub>@NiO core-shell NPs. A two-step process is employed. First, TiO<sub>2</sub> core NPs are prepared via solution plasma in the presence of PVP. Then, NiO shell NPs are introduced onto the PVP-encapsulated TiO<sub>2</sub> NPs in the same solution using solution plasma. The effect of PVP concentration on NP formation and structure was investigated. The size, surface morphology, elemental composition, crystalline structure and surface information of the NPs were also explored.

#### 2. Experimental

**Materials.** All materials were obtained from local commercial suppliers. Platinum (Pt), titanium (Ti), and nickel (Ni) wires, each with a diameter of 0.5 mm and purity range between 99.5 and 99.99 mass%, were purchased from Nilaco, Tokyo, Japan. Potassium carbonate (K<sub>2</sub>CO<sub>3</sub>) and PVP (PVP-K=30, decomposition temperature 150°C) were purchased from Kanto Chemical Co., Inc, Japan.

#### 2.1. Solution plasma setup

Fig. 1 shows the experimental setup, which consisted of two electrodes submerged in an electrolyte solution and connected to a direct-current power supply. The anode was a Pt wire with a length of 1000 mm that was coiled around a semicircular glass frame (height of 45 mm and width of 60 mm). The cathode was Ti or Ni wire with a length of 150 mm; these cathodes were used sequentially to form the desired particle structure. The cathode was shielded with a glass tube with an inner diameter of 1.1 mm to obtain an exposed length of 10 mm and the distance between the electrodes was 30 mm. The anode and cathode were cleaned using ethanol and submerged in a 300-mL glass beaker containing an electrolyte solution of 0.1 M  $K_2CO_3$  (300 mL, pH 12) mixed with PVP (0 to 0.25% (w/v)). The solution was warmed

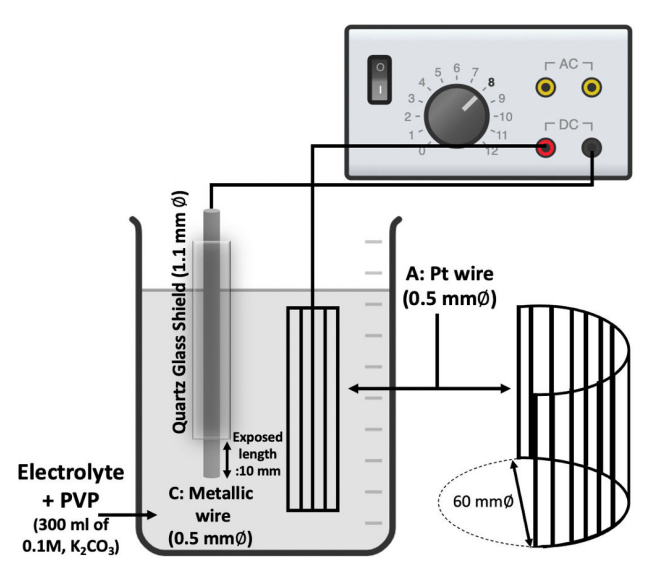


Fig. 1. Solution plasma setup

from room temperature to  $80 \pm 3$  °C using a hotplate with a magnetic stirrer. The glow-discharge plasma generated around the cathode was sustained by applying voltage from a direct-current power supply (Kikusui PWR1600L, Japan).

# 2.2. Core-shell nanoparticles synthesis and collection

The core-shell NPs were synthesized in K<sub>2</sub>CO<sub>3</sub> solution with different PVP concentrations (TABLE 1). Synthesis parameters such as the applied voltage, current, and electrolysis time were summarized in TABLE 2. The TiO<sub>2</sub>@NiO core-shell NPs were prepared as follows. First, TiO<sub>2</sub> core NPs were produced by discharging the Ti wire in the K<sub>2</sub>CO<sub>3</sub> solution with the lowest concentration of PVP until plasma formed at a rate of 0.5 V/min from 0.0 V. Then, the voltage was fixed at a constant value for 1 hour. Second, the Ti wire was replaced with Ni wire to deposit the NiO shell NPs in the same solution by solution plasma using the specified voltage and time, as represented in Fig. 2. The experiment was repeated with different concentrations of PVP. After synthesis, the NPs were collected via centrifugation and washed with deionized water to remove the electrolyte and excess PVP; this process was repeated four times.

TABLE 1
The concentration of polyvinylpyrrolidone (PVP) in percentage weight/volume % (w/v) and grams (g)

Concentration of PVP % (w/v)	Grams (g)
0	0
0.05	0.15
0.15	0.45
0.25	0.75

TABLE 2
Synthesis parameters of titanium (Ti) and nickel (Ni) wire for TiO<sub>2</sub>@NiO core-shell NPs using solution plasma

Applied Voltage (V)		Current (A)		Electrolysis Time (min)	
Ti	Ni	Ti	Ni	Ti	Ni
110	130	0.41	0.36	60	60

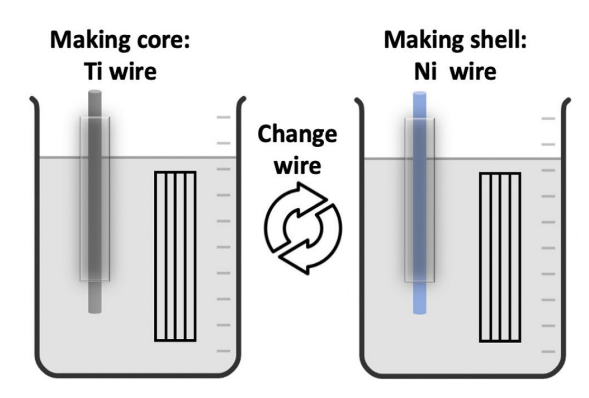


Fig. 2. TiO<sub>2</sub>@NiO core-shell NPs synthesis method

#### 2.3. Core-shell nanoparticles analysis method

The yield of NPs obtained was evaluated by measuring the average mass of the cathode wire before and after the solution plasma process using an analytical balance (Mettler Toledo, XSR104). Samples were characterized by X-ray diffractometer (XRD, Rigaku Miniflex II, Cu-Kα source) over a scan range of  $2\theta = 20^{\circ} - 80^{\circ}$  to identify phases. The morphology of NPs was observed by field-emission scanning electron microscopy (SEM, JEOL JSM-7001FA), scanning transmission electron microscopy (STEM, JEOL JEM-ARM200F NEOARM) and transmission electron microscopy (TEM, JEOL JEM-2100). The aqueous solution containing the NPs was deposited onto a silicon wafer and a Quantifoil grid (a type of perforated support foil) for SEM, STEM and TEM observation. Elemental composition was determined using energy-dispersive X-ray spectroscopy (EDS). The particles size distribution was estimated using ImageJ software. Elemental analysis of the surface and chemical state was identified using X-ray photoelectron spectroscope (XPS, JEOL JPS-9200, Al-Kα source). The binding energy was corrected with reference to the C 1s peak (285 eV) for the samples prepared. Dried NPs powder was deposited onto adhesive carbon tape for XPS analysis.

#### 3. Results and discussion

## 3.1. Nanoparticle yield

The average yield of the core-shell NPs formed using different PVP concentrations after 1 h of solution plasma treatment is presented in Fig. 3. The yield of NPs produced using the Ni wire was higher than that produced using the Ti wire. The higher voltage applied to the Ni wire than the Ti wire during the solution plasma process was viewed as the primary cause of this difference. At higher voltages, the increased current concentration effect and Joule heating accelerate cathode melting and, consequently, forming more of NPs.

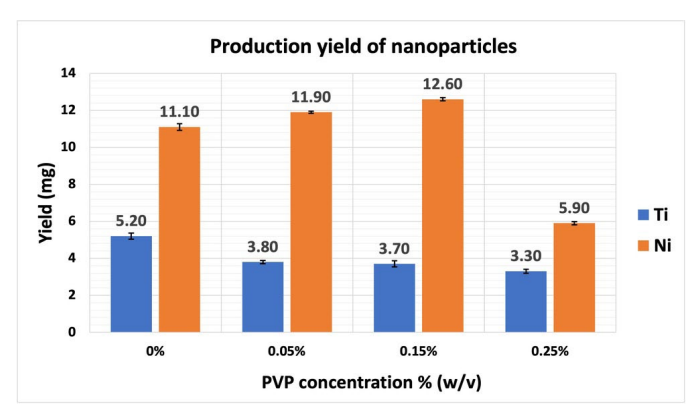


Fig. 3. The yield of NPs in milligrams (mg) relative to the PVP concentrations % (w/v) from Ti and Ni wire

The yield of NPs was affected by the PVP concentration. The highest yields with PVP were obtained at PVP concentrations

of 0.05% and 0.15% (w/v), whereas the lowest was recorded at 0.25% PVP for both materials. The quantity of NPs produced by the Ti wire decreased with increasing PVP concentration. In contrast, PVP concentration had little effect on the yield of NPs produced using Ni wire. This is attributed to the interaction of PVP with the plasma; the increase in viscosity caused by PVP resulted in the lower production of particles at low voltages but had little effect at high voltages. A PVP concentration of 0.25% (w/v) gave the lowest yield because the high solution viscosity hindered NP formation.

#### 3.2. XRD analysis

The XRD patterns in Fig. 4 show the elemental composition of the NPs synthesized using different PVP concentrations. The diffraction patterns contained well-defined peaks corresponding to TiO<sub>2</sub> (oxygen-deficient, anatase and rutile phases) as well as peaks consistent with Ni and NiO. The anatase phase of TiO<sub>2</sub> showed peaks at  $2\theta = 24.44^{\circ}$  and 55.71°, which were attributed to the (101) and (211) planes, respectively (ICDD card No. 00-021-1272), whereas the rutile phase showed peaks at  $2\theta = 35.70^{\circ}$ ,  $40.81^{\circ}$ and 53.81°, which were ascribed to the (101), (111) and (211) planes, respectively (ICDD card No. 00-021-1276). Both phases had a tetragonal crystal structure. Additional peak located at ~28.89° were identified as oxygen-deficient phase (ODP) of TiO<sub>2</sub>. ODP is recognized as the absence of some oxygen atom compared with the normal stoichiometric TiO<sub>2</sub> [15]. Moreover, Ni exhibited peaks at  $2\theta = 44.25^{\circ}$ ,  $51.61^{\circ}$  and  $76.15^{\circ}$ , which were attributed to the (111), (200), and (220) planes of the cubic crystal structure, respectively (ICDD card No. 00-004-0850). NiO displayed peaks at  $2\theta = 37.09^{\circ}$ ,  $43.14^{\circ}$ ,  $62.81^{\circ}$  and  $74.62^{\circ}$ , that were ascribed to the (111), (200), (220), and (311) planes of the cubic structure, respectively (ICDD card No. 00-047-1049).

The XRD results demonstrated that the addition of PVP did not affect the composition of the products. Intense Ni and NiO

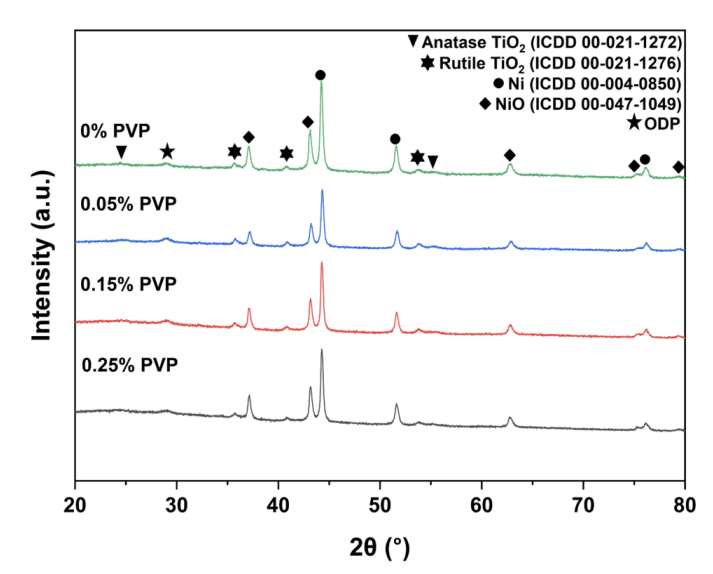


Fig. 4. X-ray diffraction (XRD) patterns of  $TiO_2@Ni/NiO$  core-shell NPs at different PVP concentrations % (w/v)

peaks were observed, suggesting a larger amount of these phases than that of TiO<sub>2</sub> because of the higher voltage applied in the second solution plasma step than in the first. Ni peaks emerged due to the properties of the material forming a passivation layer (a nickel oxide layer) on the surface of the particles when exposed to an oxidizing environment such as that of submerged glow discharge plasma, thus preventing further oxidation [16]. Because Ni was present in both its pure metallic and oxide form in the shell NPs, they will hereafter be referred to as Ni/NiO NPs.

## 3.3. SEM and EDS analyses

Fig. 5 presents high-magnification SEM and EDS images of the NPs. In terms of morphology, both TiO<sub>2</sub> and Ni/NiO NPs possessed smooth surfaces and were spherical. The EDS mapping images confirmed the presence of an oxide layer on the NP surface, indicating both Ti and Ni existed as oxides. The effect of PVP concentration on NP morphology and composition was investigated by comparing SEM and EDS results for the sample produced without PVP with those of samples formed in the presence of PVP (0.05%, 0.15%, and 0.25% (w/v)). The results indicated that PVP facilitates the attachment of the smaller Ni/NiO shell NPs onto the surface of the larger TiO<sub>2</sub> core particles through its binding effect, which likely originates from the polar

amide group (–NH–CO–) of PVP [17]. However, the coverage of the TiO<sub>2</sub> core particles with Ni/NiO shell NPs was partial and inhomogeneous throughout the samples. In fact, distinguishing which PVP concentration provided the most uniform coverage of shell materials was challenging because of the inconsistent attachment of shell NPs to the core surface. The uneven ratio of core-shell NPs during production, plasma conditions, and application method of the surface modifier (PVP) are believed to contribute to the nonuniform shell formation. Therefore, the particles will hereafter be referred to as quasi core-shell nanoparticles. From these results, it can be deduced that the addition of PVP facilitates adhesion of Ni/NiO NPs on the TiO<sub>2</sub> NPs, suggesting that PVP strengthened the interaction between the two types of NPs by acting as a binding agent.

### 3.4. Average quasi core-shell nanoparticle size

The average size distributions of the particles measured in the SEM images are shown as histograms in Fig. 6. In terms of particle size, the average diameter of  $TiO_2$  NPs was  $590 \pm 49$  nm and that of Ni/NiO NPs was  $260 \pm 16$  nm for the sample formed without PVP. With the addition of PVP (0.05%, 0.15%, and 0.25% (w/v)), the average diameter of the  $TiO_2$  NPs ranged from 600 to 670 nm and that of Ni/NiO NPs was from 200

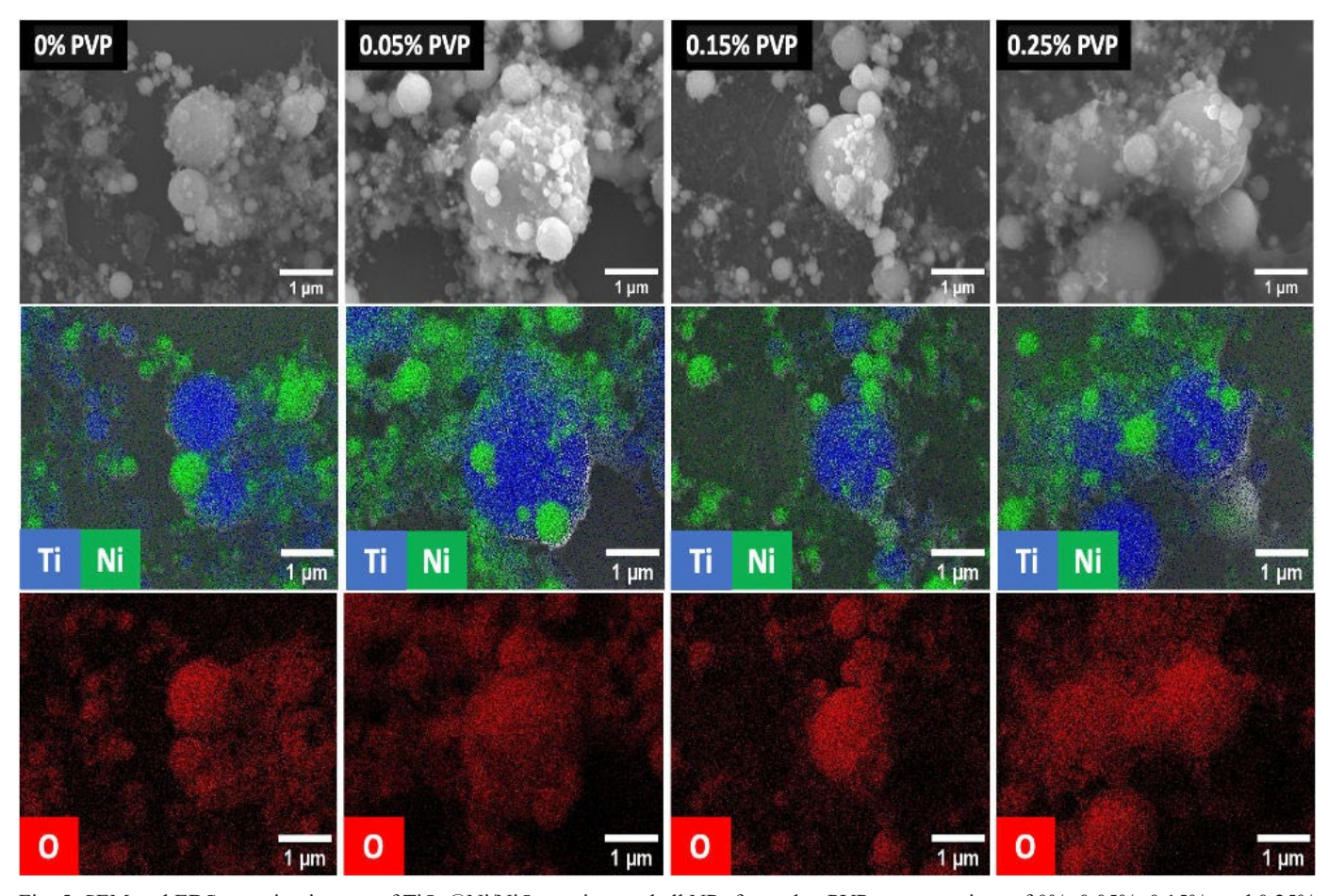


Fig. 5. SEM and EDS mapping images of TiO<sub>2</sub>@Ni/NiO quasi core-shell NPs formed at PVP concentrations of 0%, 0.05%, 0.15%, and 0.25% (w/v) (from left to right)

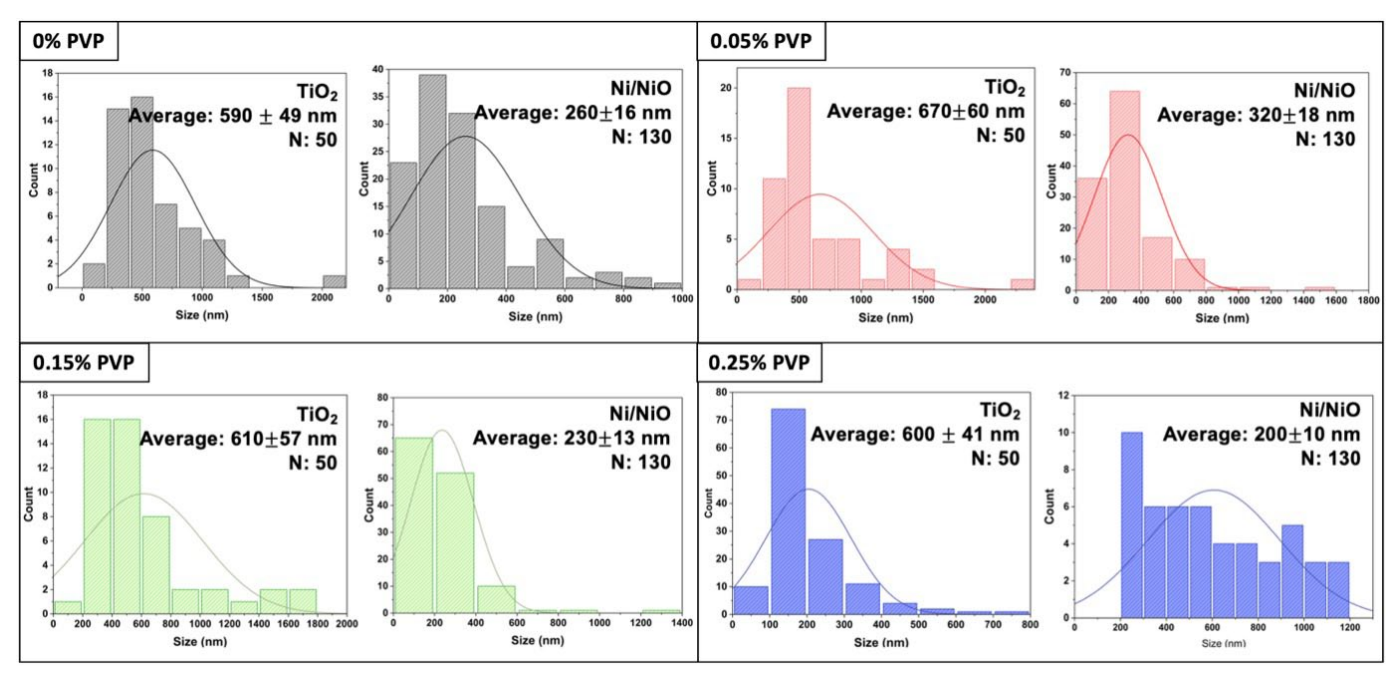


Fig. 6. Particles size distributions of TiO<sub>2</sub>@Ni/NiO quasi core-shell NPs formed at PVP concentrations of 0%, 0.05%, 0.15%, and 0.25% (w/v)

to 320 nm. On the basis of the histograms, the influence of applied voltage on the particle size is evident. The higher voltage applied to the Ni wire (130 V) generated smaller particles and the lower voltage applied to the Ti wire (110 V) produced larger particles. Furthermore, PVP influences the size of NPs formed. Initially, the introduction of PVP at 0.05% (w/v) increase the size of particles for both Ti and Ni/NiO NPs, later decrease with higher concentration of PVP (0.15% and 0.25% (w/v)). For example, the sample produced using 0.05% PVP had average NPs sizes of  $670 \pm 60$  nm and  $320 \pm 18$  nm for TiO<sub>2</sub> and Ni/NiO NPs, respectively, whereas the sample produced using 0.25% PVP had average NPs sizes of  $600 \pm 41$  nm and  $200 \pm 10$  nm for TiO<sub>2</sub> and Ni/NiO NPs, respectively. The properties of PVP as stabilizer control the size of particles produced, resulting in a smaller particle size for both materials [18].

#### 3.5. STEM, TEM and EDS analyses

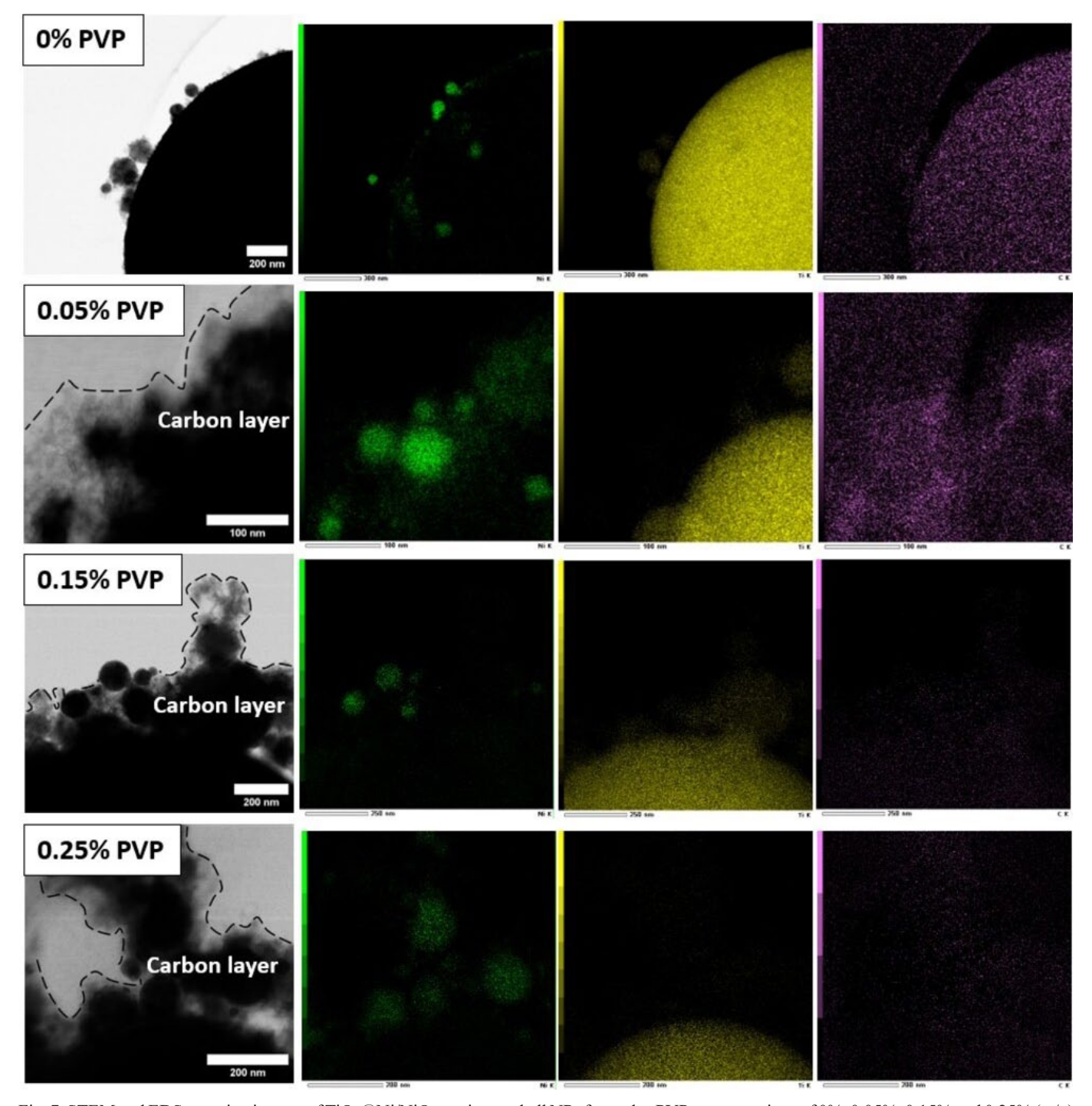
Fig. 7 shows STEM images of the TiO<sub>2</sub>@Ni/NiO quasi core-shell NPs produced using different PVP concentrations. The NPs were uniformly spherical in shape, which was consistent with the SEM results. Without PVP, the particles did not exhibit a clear core-shell structure; rather, small Ni/NiO NPs appear to surround the large TiO<sub>2</sub> NPs. When 0.05% (w/v) PVP was included, Ni/NiO shell tends to form a more tightly bound layer around TiO<sub>2</sub> cores, suggesting a well-defined quasi coreshell structure. The carbon mapping further indicates the presence of PVP layer on the surface of the NPs. Upon increasing the PVP concentration to 0.15% (w/v), the TiO<sub>2</sub>@Ni/NiO quasi core-shell NPs were also noticeable, indicating that both 0.05% and 0.15% PVP concentrations provide optimal conditions for forming NPs with a quasi core-shell structure. At the highest

concentration of PVP of 0.25% (w/v), quasi core–shell structure was observable, however, the sample was overconcentrated with PVP, as shown in Fig. 8(a). TEM images in Fig. 8(b) also revealed by-products from PVP degradation. At this PVP concentration, the combination of the high-temperature environment of the solution plasma process, low decomposition temperature of PVP, and high solution viscosity led to the degradation of PVP, producing visible solid precipitates as a by-product. The degradation of PVP may have occurred through the random chain scission mechanism [19]. PVP degradation interfered with NPs formation and hindered the development of quasi core-shell structure.

## 3.6. XPS analysis

Fig. 9(a) shows the full XPS spectrum of  $TiO_2@Ni/NiO$  quasi core-shell NPs prepared with different PVP concentrations. The spectrum of NPs reveals the main peaks at binding energies of about 865.0, 531.0, 458.0, and 285.0 eV, corresponding with Ni 2p, O 1s, Ti 2p, and C 1s, respectively . Notably, a peak at 400.0eV of N 1s was clearly observed only in sample containing PVP, confirming its presence on the NPs surface. The N 1s signal is ascribed to nitrogen (N) atom in the pyrrolidone group of PVP polymer [20,21].

For accurate surface analysis of the TiO<sub>2</sub>@Ni/NiO quasi core-shell NPs, only high resolution XPS spectrum of N 1s was focused as the O 1s and C 1s signals may originate from PVP or residual organic solvents. Fig. 9(b) shows the high resolution XPS spectra of N 1s. The N 1s peak represents the contribution of nitrogen in PVP. Only one peak was detected for each sample containing PVP at binding energies: 400.1, 399.3, 399.5 eV for 0.05%, 0.15% and 0.25% PVP, respectively.



 $Fig.~7.~STEM~and~EDS~mapping~images~of~TiO_2@Ni/NiO~quasi~core-shell~NPs~formed~at~PVP~concentrations~of~0\%, 0.05\%, 0.15\%~and~0.25\%~(w/v)~images~of~TiO_2@Ni/NiO~quasi~core-shell~NPs~formed~at~PVP~concentrations~of~0\%, 0.05\%, 0.05\%, 0.05\%~(w/v)~images~of~TiO_2@Ni/NiO~quasi~core-shell~NPs~formed~at~pvP~concentrations~of~0\%, 0.05\%, 0.05\%, 0.05\%~(w/v)~images~of~TiO_2@Ni/NiO~quasi~core-shell~NPs~formed~at~pvP~concentrations~of~0\%, 0.05\%, 0.05\%, 0.05\%, 0.05\%~(w/v)~images~of~TiO_2@Ni/NiO~quasi~core-shell~NPs~formed~at~pvP~concentrations~of~0\%, 0.05\%, 0.05\%, 0.05\%, 0.05\%, 0.05\%~(w/v)~images~of~0\%, 0.05\%$ 

The shift of N 1s peak to lower binding energies is attributed to the strong chemisorption on the surface of Ti and Ni/NiO, originated from electronic donor-acceptor interactions [22]. Thus, the results indicate strong PVP-NPs surface interactions, contributing to the formation of  $TiO_2@Ni/NiO$  quasi core-shell NPs.

#### 4. Conclusion

 ${\rm TiO_2@Ni/NiO}$  quasi core-shell NPs were synthesized through a solution process with different concentrations of

PVP. XRD analysis confirmed that the samples contained  $TiO_2$  (oxygen-deficient, anatase and rutile phases), Ni, and NiO. The NPs were smooth and spherical, with  $TiO_2$  partially covered by Ni/NiO particles when PVP was present. The addition of PVP facilitated adhesion of the smaller Ni/NiO NPs on the larger  $TiO_2$  NPs surface, suggesting PVP acted as a binding agent. The  $TiO_2$  NPs were larger than the Ni/NiO NPs because of the different voltages applied during the two-steps of the solution plasma process. XPS analysis further supports the interaction PVP with NPs surface by N 1s peak, facilitating the formation of  $TiO_2@Ni/NiO$  quasi core-shell NPs. The optimal PVP concentration to

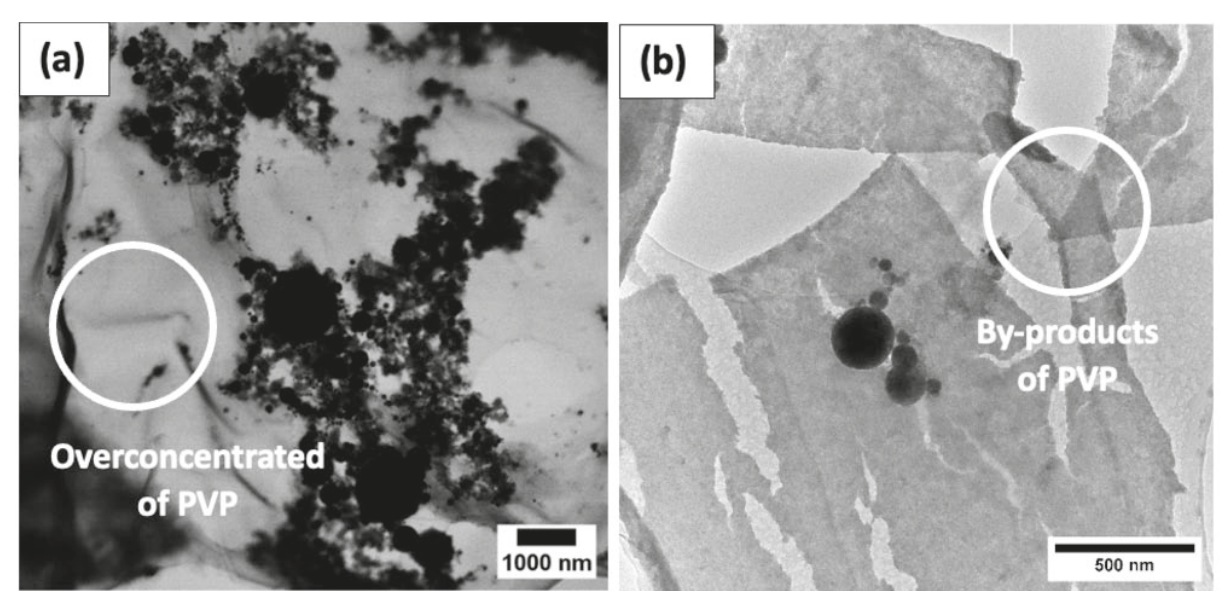


Fig. 8. (a) STEM image of overconcentrated PVP at 0.25% (w/v) and (b) TEM image of PVP by-products at 0.25% (w/v)

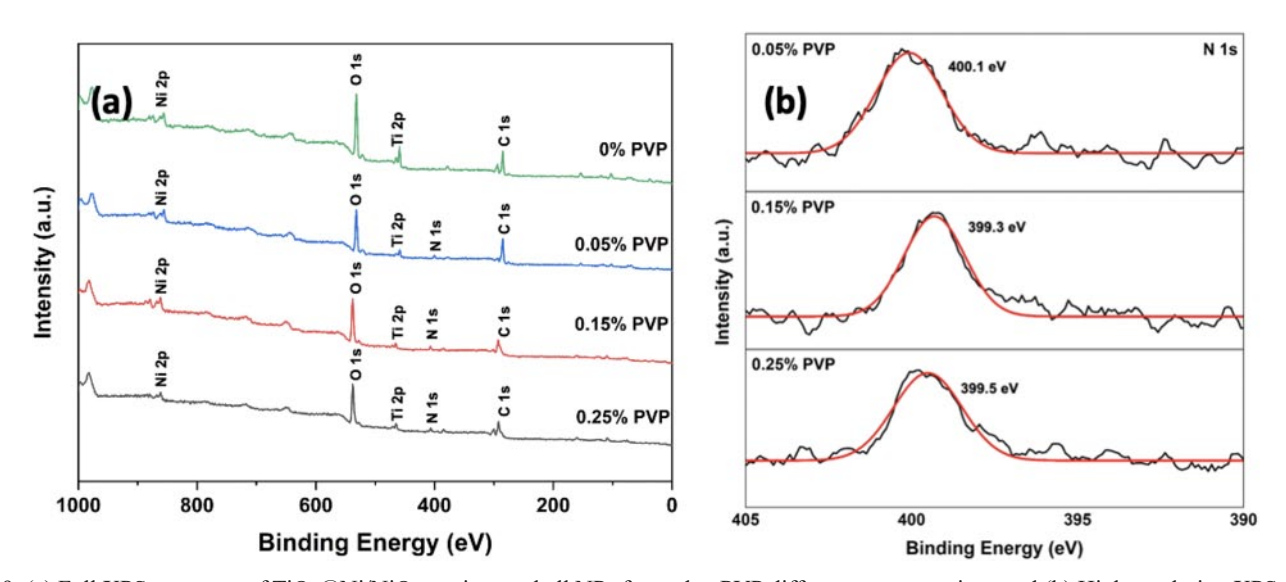


Fig. 9. (a) Full XPS spectrum of TiO<sub>2</sub>@Ni/NiO quasi core-shell NPs formed at PVP different concentrations and (b) High resolution XPS spectrum of N 1s

promote core-shell NP formation was around 0.05% to 0.15% (w/v). A high PVP concentration of 0.25% (w/v) led to overconcentrated and degradation of PVP and suppressed the formation of core-shell NP structure. Although the formation mechanism of core-shell NPs in the presence of PVP is not yet fully understood, these findings reveal the potential of solution plasma using an appropriate surface modifier for synthesis of core-shell NPs.

#### Acknowledgement

The work was supported by Advanced Research Infrastructure for Materials and Nanotechnology in Japan (ARIM)" of the Ministry of Education, Culture, Sports, Science and Technology (MEXT), grant number JPMX-P1224HK0013 (Hokkaido University). The authors would like to express special thanks to Kenji Ohkubo, Takashi Tanioka, Ryoko Yokohira, Keita

Suzuki for their technical assistance with SEM, STEM, TEM and XPS observations. We also thank Natasha Lundin, PhD, from Edanz (https://jp.edanz.com/ac) for editing a draft of this manuscript. Their contributions are sincerely appreciated and gratefully acknowledged. The results were presented during the 14th Polish Japanese Joint Seminar on Micro and Nano Analysis (3-6.09.2024, Toyama, Japan

# REFERENCES

[1] D.O. Scanlon, C.W. Dunnill, J. Buckeridge, S.A. Shevlin, A.J. Logsdail, S.M. Woodley, C.R.A. Catlow, M.J. Powell, R.G. Palgrave, I.P. Parkin, G.W. Watson, T.W. Keal, P. Sherwood, A. Walsh, A.A. Sokol, Band alignment of rutile and anatase TiO<sub>2</sub>. Nat. Mater. 12 (9), 798-801 (2013).

DOI: https://doi.org/10.1038/nmat3697

- [2] A. Uma Maheswari, K. K. Anjali, M. Sivakumar, Optical absorption enhancement of PVP capped TiO<sub>2</sub> nanostructures in the visible region. Solid State Ionics 337, 33-41 (2019).
  DOI: https://doi.org/10.1016/j.ssi.2019.04.001
- [3] A. Fujishima, K. Honda, Electrochemical Photolysis of Water at a Semiconductor Electrode. Nature 238, 37-38 (1972).
   DOI: https://doi.org/10.1038/238037a0
- [4] M.A. Mannaa, K.F. Qasim, F.T. Alshorifi, S.M. El-Bahy, R.S. Salama, Role of NiO Nanoparticles in Enhancing Structure Properties of TiO<sub>2</sub> and Its Applications in Photodegradation and Hydrogen Evolution. ACS Omega 6 (45), 30386-30400 (2021). DOI: https://doi.org/10.1021/acsomega.1c03693
- [5] N.J. Baygi, A.V. Saghir, S.M. Beidokhti, J.V. Khaki, Modified auto-combustion synthesis of mixed-oxides TiO<sub>2</sub>/NiO nanoparticles: Physical properties and photocatalytic performance. Ceram. Int. 45 (10), 15417-15437 (2020). DOI: https://doi.org/10.1016/j.ceramint.2020.03.087
- [6] H. Zhao, C.F. Li, L.Y. Liu, B. Palma, Z.Y. Hu, S. Renneckar, S. Larter, Y. Li, M.G. Kibria, J. Hu, B.L. Su, n-p Heterojunction of TiO<sub>2</sub>-NiO core-shell structure for efficient hydrogen generation and lignin photoreforming. J. Colloid Interface Sci. 585, 694-704 (2021). DOI: https://doi.org/10.1016/j.jcis.2020.10.049
- [7] P. Rana, P. Jeevanandam, A Facile Synthetic Approach for TiO<sub>2</sub>@ NiO Core-shell Nanoparticles using TiO<sub>2</sub>@Ni(OH)<sub>2</sub> Precursors and their Photocatalytic Application. ChemNanoMat. 10 (3), 1-11 (2024). DOI: https://doi.org/10.1002/cnma.202300481
- [8] Y. Toriyabe, S. Watanabe, S. Yatsu, T. Shibayama, T. Mizuno, Controlled formation of metallic nanoballs during plasma electrolysis. Appl. Phys. Lett. 91, 041501 (2017). DOI: https://doi.org/10.1063/1.2760042
- [9] G. Saito, S. Hosokai, M. Tsubota, T. Akiyama, Synthesis of copper/copper oxide nanoparticles by solution plasma. J. Appl. Phys. 110 (2), 023302 (2011).
   DOI: https://doi.org/10.1063/1.3610496
- [10] M.R.M. bin Julaihi, S. Yatsu, M. Jeem, S. Watanabe, Synthesis of stainless steel nanoballs via submerged glow-discharge plasma and its photocatalytic performance in methylene blue decomposition. J. Exp. Nanosci. 10 (12), 965-982 (2015). DOI: https://doi.org/10.1080/17458080.2014.951408
- [11] G. Saito, S. Hosokai, M. Tsubota, T. Akiyama, Nickel Nanoparticles Formation from Solution Plasma Using Edge-Shielded Electrode. Plasma Chem. Plasma Process. 31 (5), 719-728 (2011). DOI: https://doi.org/10.1007/s11090-011-9313-4
- [12] H. Sun, J. He, J. Wang, S.Y. Zhang, C. Liu, T. Sritharan, S. Mhaisalkar, M.Y. Han, D. Wang, H. Chen, Investigating the multiple

- roles of polyvinylpyrrolidone for a general methodology of oxide encapsulation. J. Am. Chem. Soc. **135** (24), 9099-9110 (2013). DOI: https://doi.org/10.1021/ja4035335
- [13] A. Tiwari, A.K. Tripathi, P. Khare, A comprehensive study of synthesis and applications of core/shell nanoparticles. Int. J. Eng. Sci. Technol. 13 (1), 153-157 (2021). DOI: https://doi.org/10.4314/ijest.v13i1.23s
- [14] K.M. Koczkur, S. Mourdikoudis, L. Polavarapu, S.E. Skrabalak,
   Polyvinylpyrrolidone (PVP) in nanoparticle synthesis. Dalt. Trans.
   44 (41), 17883-17905 (2015).
   DOI: https://doi.org/10.1039/c5dt02964c
- [15] S. Zhu, Z. Yu, L Zhang, S, Watabe, Solution Plasma-Synthesized Black TiO2Nanoparticles for Solar-Thermal Water Evaporation. ACS Appl. Nano Mater. 4 (4), 3940-3948 (2021). DOI: https://doi.org/10.1021/acsanm.1c00322
- [16] P. Song, D. Wen, Z.X. Guo, T. Korakianiti, Oxidation investigation of nickel nanoparticles. Phys. Chem. Chem. Phys. 10 (33), 5057-5065 (2008).
  DOI: https://doi.org/10.1039/B800672E
- [17] G. Jian, C. Zhang, C. Yan, K.S. Moon, C.P. Wong, Scalable Preparation of Fully Coated Ag@BaTiO<sub>3</sub> Core@Shell Particles via Poly(vinylpyrrolidone) Assistance for High-k Applications. ACS Appl. Nano Mater. 1 (3), 1396-1405 (2018). DOI: https://doi.org/10.1021/acsanm.8b00220
- [18] R. Zein, I. Alghoraibi, C. Soukkarieh, M.T. Ismail, A. Alahmad, Influence of Polyvinylpyrrolidone Concentration on Properties and Anti-Bacterial Activity of Green Synthesized Silver Nanoparticles. Micromachines 13 (5) (2022). DOI: https://doi.org/10.3390/mi13050777
- [19] Akyüz, M. Özkan, Degradation of polyvinylpyrrolidone by solution plasma process. Acta Phys. Pol. A. 131 (3), 343-345 (2017). DOI: https://doi.org/10.12693/APhysPolA.131.343
- [20] I. Shepa, E. Mudra, D. Pavlinak, V.Antal, J. Bednarcik, O. Mikovic, A. Kovalcikova, J. Dusza, Surface Plasma Treatment of the Electrospun TiO2/PVP Composite Fibers in Different Atmospheres. Appl. Surf. Sci. 523 (2020).
  DOI: https://doi.org/10.1016/j.apsusc.2020.146381
- [21] D. Özhava, N.Z. Kiliçaslan, S. Özkar, PVP-Stabilized Nickel(0) Nanoparticles as Catalyst in Hydrogen Generation from the Methanolysis of Hydrazine Borane or Ammonia Borane. Appl. Catal. B Environ. 162, 573-582 (2015). DOI: https://doi.org/10.1016/j.apcatb.2014.07.033
- [22] I. A. Safo, M.Werheid, C. Dosche, M. Oezaslan, The Role of Polyvinylpyrrolidone (PVP) as a Capping and Structure-Directing Agent in the Formation of Pt Nanocubes. Nanoscale Adv. 1 (8), 3095-3106 (2019). DOI: https://doi.org/10.1039/c9na00186g